Article

Not peer-reviewed version

Development of a Particle-Free Linear Atmospheric Plasma Device for Hydrophilization of Silicon Wafers

Sho Yoshida , Koki Hihara , Junnosuke Furuya , Taiki Osawa , Akane Yaida , Nobuhiko Nishiyama , Akitoshi Okino *

Posted Date: 18 August 2025

doi: 10.20944/preprints202508.1235.v1

Keywords: atmospheric plasma; particle-free; hydrophilization; linear plasma device; semiconductor manufacturing process

 doi:10.20944/preprints202508.1235.v1

Article

Development of a Particle-Free Linear Atmospheric Plasma Device for Hydrophilization of Silicon Wafers

Sho Yoshida [1], Koki Hihara [1], Junnosuke Furuya [1], Taiki Osawa [1], Akane Yaida [1], Nobuhiko Nishiyama [2] and Akitoshi Okino [1,*]

[1] FIRST, Institute of Innovative Research, Institute of Science Tokyo, J2-32, 4259 Nagatsuta, Midori-ku, Yokohama 226-8501, Japan

[2] Department of Electrical and Electronic Engineering, Institute of Science Tokyo, Building No. 9, Ookayama Minami, 1-31 Ishikawa-cho, Ota City, Tokyo 145-0061, Japan

* Correspondence: aokino@first.iir.isct.ac.jp ; Tel.: +81-45-924-5688

Abstract

We developed a particle-free linear atmospheric plasma device for hydrophilizing silicon wafers, aiming to improve semiconductor manufacturing processes. The device generates a stable plasma curtain using argon or helium gas under specific frequency and power conditions, enabling large-area surface treatment without causing damage. Experimental results demonstrated uniform hydrophilization, characterized by a substantial reduction in water contact angle and minimal particle emission, outperforming conventional jet-type plasma systems. TOF-SIMS analysis confirmed the absence of metal contamination, validating the device's cleanliness. This technology offers a promising alternative to wet chemical treatments, contributing to environmentally friendly and efficient wafer bonding processes.

Keywords: atmospheric plasma; particle-free; hydrophilization; linear plasma device; semiconductor manufacturing process

1. Introduction

Atmospheric plasma, which can be operated in open systems without the need for vacuum pumps or exhaust equipment, enables high-density and continuous treatment of reactive species. This characteristic has led to its application across various industrial fields, including semiconductor processing [1–3], decomposition of hazardous gases [4], detoxification of harmful substances [5], and elemental analysis [6–10]. Furthermore, advancements in plasma temperature control technologies [11] have expanded its potential use in medical devices [12] and sterilization processes [13].

Semiconductor devices are essential to modern society, particularly integrated circuits, which are indispensable in communication, computing, and energy management. As global data traffic continues to increase annually, concerns regarding rising energy consumption and greenhouse gas emissions have intensified [14]. Enhancing the performance of semiconductor devices is considered one of the key solutions to these challenges. In semiconductor manufacturing, plasma processes play a crucial role in pattern formation via etching, dielectric film deposition through plasma Chemical Vapor Deposition, and wafer bonding via hydrophilization and contaminant removal. Historically, performance improvements have been achieved primarily through advancements in processing technologies for single-material systems such as silicon. However, the limitations of such approaches have become increasingly apparent [15–18]. Recent research has focused on photonic devices, which offer ultra-low power consumption and ultra-wide bandwidth capabilities [19–21]. In developing

 doi:10.20944/preprints202508.1235.v1

these devices, heterogeneous integration of silicon with III–V compound semiconductors has been proposed, enabling the realization of high-performance optical communication devices [22–24]. Heterogeneous integration refers to the fabrication of integrated circuits by optimally combining multiple semiconductor materials with distinct properties, thereby achieving device performance unattainable with single-material systems. This approach is especially important for optical communication applications.

Hydrophilic bonding has been proposed for joining dissimilar semiconductor materials. Traditionally, wet chemical treatments using oxidizing agents have been employed, but these require waste liquid treatment facilities and high-temperature annealing, prompting the need for simpler methods [25,26]. Recently, dry bonding techniques using low-pressure plasma in vacuum chambers have gained attention [27–29]. However, these methods involve complex processes and pose challenges for productivity [30–34]. Consequently, efforts have been made to simplify bonding processes by utilizing atmospheric plasma for hydrophilization.

Jet-type atmospheric plasma devices are commonly used, but they suffer from issues such as particle contamination due to electrode erosion, which can degrade cleanroom environments and device performance. Additionally, their narrow treatment width limits productivity [35]. To address these challenges, we have developed a novel linear-type plasma device with reduced particle generation. This device overcomes the limitations of conventional atmospheric plasma systems and enables inline integration with other bonding processes.

In this study, we describe the newly developed particle-free linear plasma generation device and present experimental results evaluating its performance. Specifically, we report on the particle content within the plasma and the effectiveness of hydrophilization. The objective of this research is to propose a new plasma treatment method using atmospheric plasma that can be integrated inline with other bonding processes, and to develop and evaluate the performance of the corresponding device. This approach aims to achieve both effective hydrophilization of silicon wafers and suppression of particle contamination, thereby enhancing the efficiency of high-performance semiconductor device manufacturing.

2. Materials and Methods

2.1. Fabrication of the Linear Plasma Device

Traditionally, large-area plasma treatment has been conducted using dielectric barrier discharge (DBD) systems, which perform direct treatment by placing the target material inside the device and activating the surface via direct discharge [36]. However, for delicate materials such as silicon wafers, there is a risk of damage from discharge, necessitating the development of remote treatment technologies that enable large-area processing while avoiding discharge-induced damage.

To address this issue, a new large-area remote plasma treatment device was designed and fabricated based on the following principles. As shown in Figure 1, plasma was generated between copper and aluminum electrodes by flowing plasma-generating gas and applying alternating voltage, resulting in capacitively coupled plasma. The plasma is sustained by secondary electrons emitted when ions accelerated by the electric field collide with the electrodes.

To ensure stable atmospheric plasma generation and minimize electrode damage, high-frequency power supplies of 13.56 MHz and 27.12 MHz were employed. At frequencies above 1 MHz, ions cannot follow the rapid changes in the electric field and become trapped in the discharge space, reducing collisions with electrodes. Consequently, plasma is maintained through ionization of gas molecules via electron collisions [37].

A slit measuring 349 mm × 1 mm was installed at the bottom of the device to emit plasma in a curtain-like fashion, enabling large-area remote treatment. As shown in Figure 2, the linear plasma device is enclosed in an aluminum housing with only the slit section machined. The housing is grounded, and plasma is generated between the internal copper electrodes. The hollow copper

 doi:10.20944/preprints202508.1235.v1

electrodes are cooled by circulating a coolant to suppress heat buildup. Additionally, a mechanism for uniform gas flow distribution is incorporated within the housing.

The housing dimensions are 53 mm in height, 405 mm in width, and 40 mm in depth. Symmetrical gas and coolant inlets are positioned on both sides, and a coaxial cable adapter is located at the center. Plasma generation was successfully achieved by flowing argon or helium gas and applying high-frequency voltage at 13.65 MHz or 27.12 MHz. The curtain-shaped plasma emitted from the slit allows for single-pass treatment of 12-inch wafers.

2.2. Performance Evaluation and Comparative Experiments

To evaluate hydrophilization performance, water contact angle measurements were conducted using the B100 instrument manufactured by Asumi Giken Co., Ltd. While additional evaluation methods such as surface free energy analysis using diiodomethane [38] and functional group analysis via X-ray Photoelectron Spectroscopy [39] were considered, this study focused on basic validation using water contact angle measurements.

The method for measuring the number of particles emitted from the plasma device is illustrated in Figure 3. The device was sealed in a clean bag (ASLAB Clean Bags 1-3254-07), and plasma was generated. The number of airborne particles inside the bag was measured using a particle counter (KC-01E, RION Co., Ltd.). Argon gas was used as the plasma-generating gas, and particles larger than 0.1 μm were removed using a filter (FUFL-915-6.35-0.1). Measurements were repeated five times, and the average values were used for analysis.

For comparison, particle emission from a conventional jet-type plasma device was also measured. This device is 85 mm in length and weighs 160 g, with a 1.5 mm gap between the high-voltage and ground electrodes. Plasma is generated by flowing gas and applying 16 kV at 50 Hz, which is emitted through a 1 mm diameter nozzle [40–42]. A schematic diagram of a conventional jet-type plasma device is presented in Figure 4. The device operates by generating plasma through high-voltage discharge between electrodes, which is subsequently expelled from the nozzle outlet.

Additionally, surface analysis of adsorbed substances after treatment with both the linear and jet-type plasma devices was conducted using Time-of-Flight Secondary Ion Mass Spectrometry (TOF-SIMS, ION-TOF GmbH, Germany).

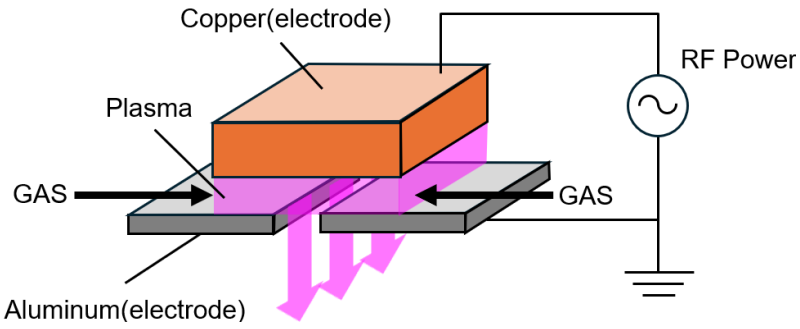

Figure 1. Method for generating large-area remote plasma.

 doi:10.20944/preprints202508.1235.v1

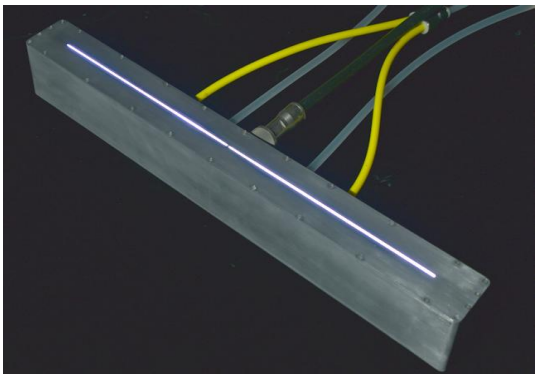

Figure 2. Developed linear plasma device.

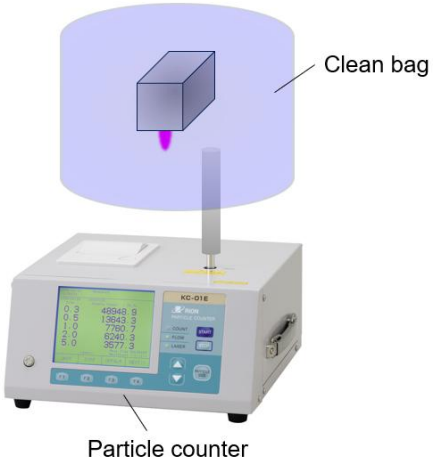

Figure 3. Method for measuring the number of particles emitted from the plasma device.

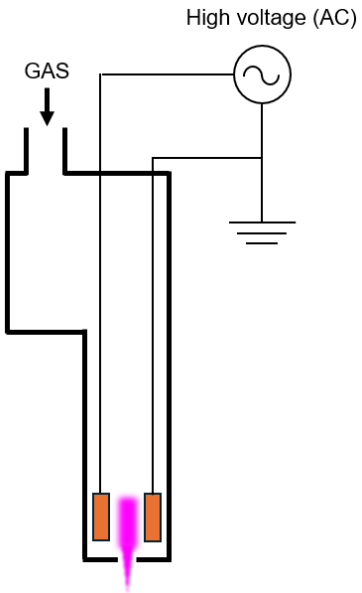

Figure 4. Schematic a conventional jet-type plasma device.

 doi:10.20944/preprints202508.1235.v1

3. Results

3.1. Conditions for Stable Plasma Generation in the Linear Plasma Device

To determine the operational conditions for stable plasma generation using the developed linear plasma device, the relationship between gas flow rate and power output was investigated for both argon and helium gases. Figure 5 illustrates the range of conditions under which stable argon plasma was generated at a frequency of 13.56 MHz. Stable plasma was observed within a gas flow rate range of 5–40 L/min and a power output range of 40–80 W. Figure 6 shows the conditions for stable helium plasma generation, which occurred within a flow rate range of 10–40 L/min and a power output range of 40–70 W. Compared to argon, helium exhibited a narrower range of stable conditions, particularly at higher flow rates where localized arc discharges were more likely to occur.

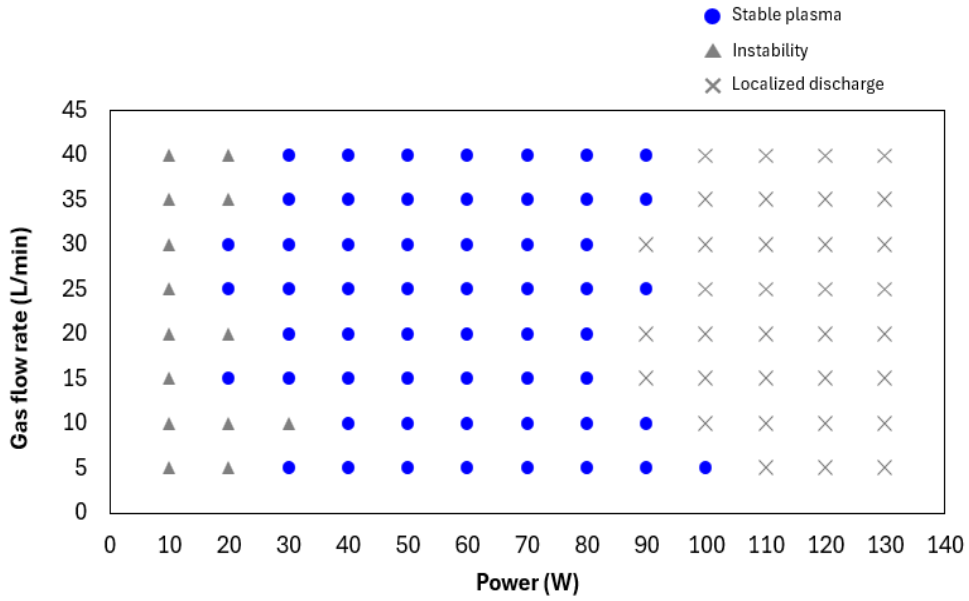

Figure 5. Conditions for stable argon plasma generation at a frequency of 13.56 MHz.

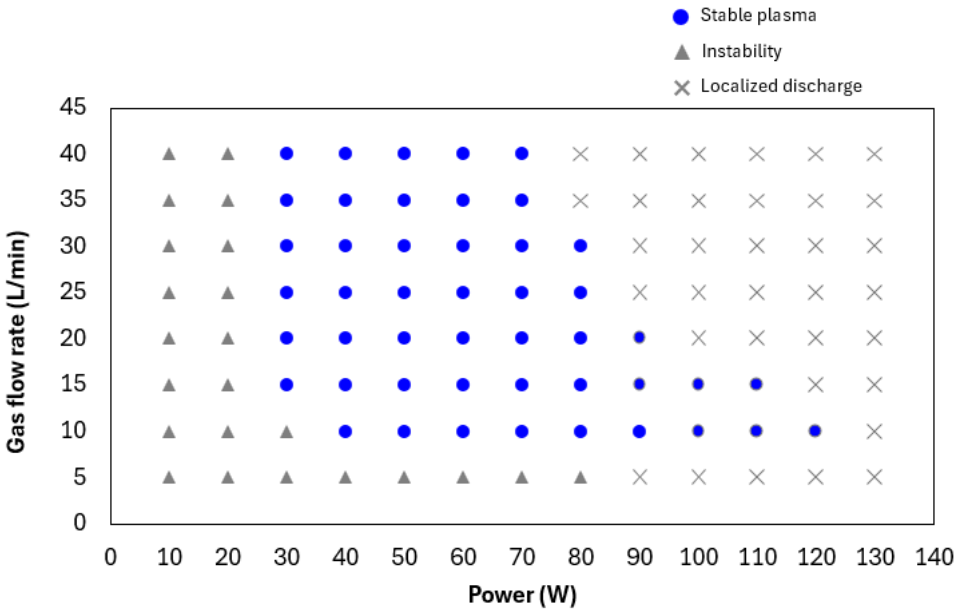

Figure 6. Range of conditions for stable plasma generation using helium gas.

 doi:10.20944/preprints202508.1235.v1

3.2. Evaluation of Hydrophilization Effect

To assess the uniformity of the plasma treatment effect, argon plasma was linearly irradiated onto silicon wafers, and hydrophilization was evaluated via contact angle measurements. Figure 7 outlines the experimental setup using the linear plasma device. The plasma was generated using a 13.56 MHz power supply at 60 W, with argon gas supplied at a flow rate of 30 L/min. The plasma was irradiated onto a 2-inch silicon wafer at a distance of 1 mm and a scanning speed of 4 mm/sec. Prior to treatment, the wafers were immersed in buffered hydrogen fluoride (BHF) for 3 minutes to remove the oxide layer and perform cleaning.To verify the uniformity of treatment across the width, five silicon wafers were arranged at 80 mm intervals, and contact angles were measured at five points per wafer. Figure 8 presents the results. The average contact angle of the cleaned wafers was 72.5°, which decreased to 13.1° after plasma treatment. The standard deviation across the width was 3.0°, indicating a high level of uniformity in hydrophilization.

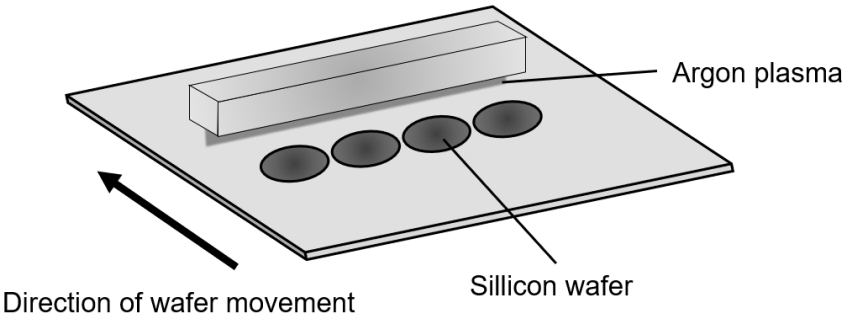

Figure 7. Experimental setup for hydrophilization of silicon using the linear plasma device.

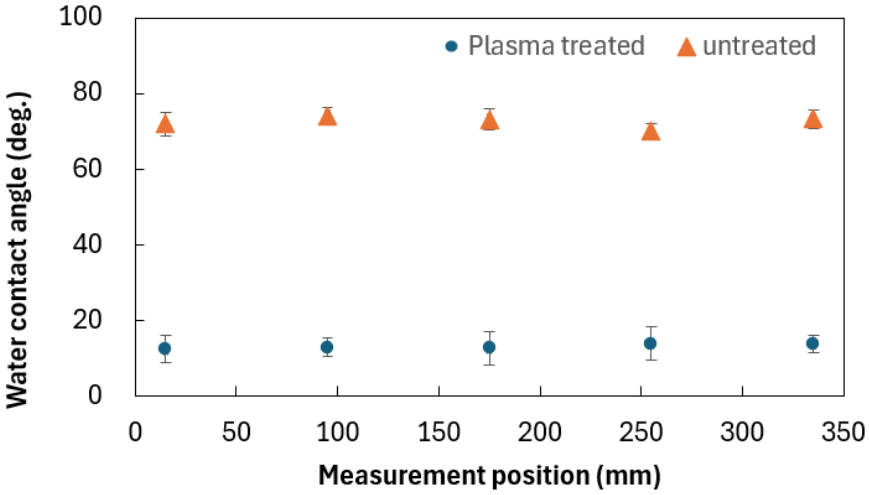

Figure 8. Hydrophilization results of silicon using the linear plasma device.

3.3. Evaluation of Particle Suppression Performance

The number of particles emitted from the linear plasma device was measured and compared with that from a conventional jet-type plasma device. The linear device operated at 27.12 MHz with an argon flow rate of 30 L/min and a power output of 165 W. The jet-type device operated at 16 kHz with an argon flow rate of 2 L/min and a voltage of 9 kV. Figure 9 shows the particle count results across various size ranges: 0.3–0.5 μm, 0.5–1 μm, 1–2 μm, 2–5 μm, and >5 μm.The jet-type device generated 5.5×10^5, 1.0×10^5, 2.3×10^4, 1.0×10^3, and 8.0 particles/L respectively in these size ranges. In contrast, the linear plasma device produced fewer than 1.0 particles/L in all size categories, demonstrating its capability as a clean plasma source.

 doi:10.20944/preprints202508.1235.v1

Figure 10 presents TOF-SIMS analysis results of silicon wafers treated by both devices. Aluminum was detected on the surface treated by the jet-type device, likely originating from electrode erosion. No significant aluminum peaks were observed on the surface treated by the linear device, indicating effective suppression of metal contamination.

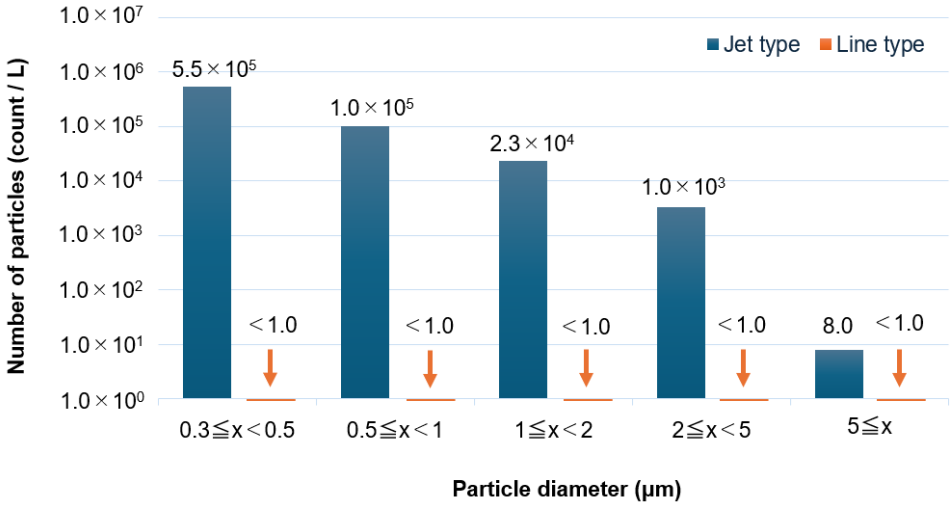

Figure 9. Particle emission from the linear plasma device.

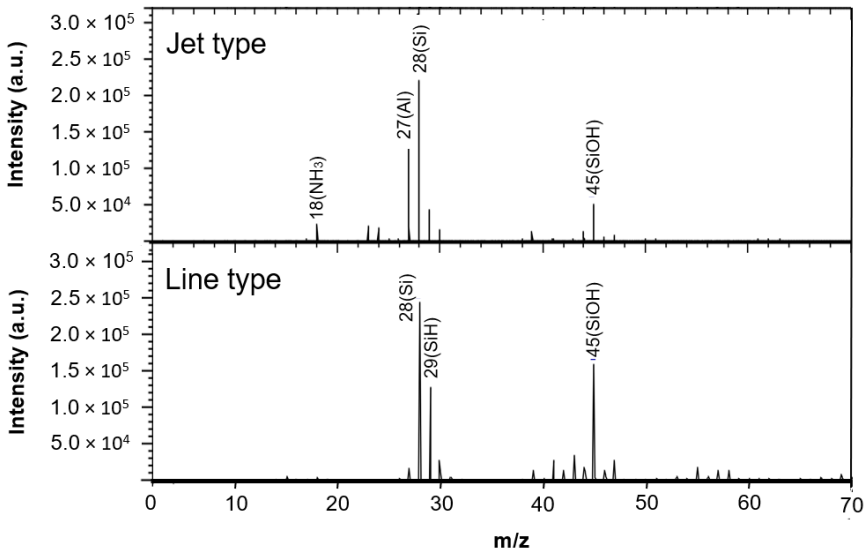

Figure 10. Chemical composition of silicon surfaces treated by jet-type and linear plasma devices.

4. Discussion

A linear-type atmospheric plasma device capable of emitting plasma in a curtain-like fashion was developed, and the conditions for stable plasma generation at a frequency of 13.56 MHz were investigated. For argon gas, stable plasma was achieved within a flow rate range of 5–40 L/min and a power range of 40–80 W. For helium gas, the stable range was narrower, with flow rates of 10–40 L/min and power outputs of 40–70 W. Although helium's higher thermal conductivity suggests more diffuse discharge, the experimental results contradicted this expectation [43,44]. Helium also has higher viscosity [45,46], which should suppress turbulent discharge [47,48]. In practice, stable plasma was generated under high-power conditions with helium. However, instability was observed at both low and high flow rates, likely due to density fluctuations in the gas stream. These fluctuations may cause instability under gravitational or acceleration fields [49,50]. Additionally, low flow rates may

 doi:10.20944/preprints202508.1235.v1

allow ambient air to mix into the plasma, further destabilizing it. Therefore, maintaining uniform flow conditions is essential for achieving stable plasma generation with helium, similar to argon.

In the hydrophilization experiments using silicon wafers, the contact angle was uniformly reduced across the entire slit width, with an average value of 13.1°. This value is comparable to those reported in previous studies [51,52], suggesting that the developed device could serve as a promising alternative. Further enhancement of hydrophilicity may be achievable by using oxygen gas or optimizing other parameters.

Particle emission measurements revealed that the developed linear plasma device did not emit detectable particles larger than 0.3 μm, indicating its suitability for cleanroom environments in semiconductor manufacturing. TOF-SIMS analysis showed no aluminum [53] contamination on the silicon wafer surface treated with the linear device, whereas aluminum was detected on wafers treated with the jet-type device. This suggests that the use of high-frequency power at 27.12 MHz reduces ion collisions with electrodes, thereby minimizing electrode erosion and particle generation.

While the device successfully generated stable atmospheric plasma across a 349 mm width and achieved uniform hydrophilization of silicon wafers, further improvements are needed for integration into semiconductor manufacturing processes. Specifically, the hydrophilization effect must be enhanced, as the contact angle achieved is higher than that of conventional low-pressure plasma treatments. Future work will focus on optimizing gas types, frequencies, and power levels to advance atmospheric plasma processing technologies.

5. Conclusions

In this study, we developed a novel particle-free linear atmospheric plasma device capable of uniformly hydrophilizing silicon wafers over a wide area. The device generates a stable plasma curtain using argon or helium gas under high-frequency conditions, enabling remote and damage-free surface treatment. Experimental results showed that the water contact angle on silicon surfaces decreased uniformly across the entire treatment width, with an average value of 13.1°. This value is comparable to those reported in previous technologies, and further improvements in hydrophilization performance are expected through optimization of gas types and processing conditions.

Moreover, particle emission measurements confirmed that the device emitted virtually no particles larger than 0.3 μm, demonstrating a significantly cleaner processing environment compared to conventional jet-type plasma devices. TOF-SIMS analysis also revealed no metal contamination on the treated silicon surfaces, validating the cleanliness of the device. These results suggest that the developed system offers a promising, environmentally friendly alternative to wet chemical treatments and is well-suited for inline processing.

Future work will focus on further enhancing hydrophilization performance and adapting the system for semiconductor manufacturing applications by investigating detailed processing parameters such as gas composition, frequency, and power. The outcomes of this research lay the foundation for next-generation atmospheric plasma technologies that combine high cleanliness and processing efficiency, contributing to the advancement of semiconductor device fabrication.

Author Contributions: Conceptualization, S.Y., A.O. and N.N.; methodology, S.Y., K.H and A.O.; investigation, S.Y., K.H., and J.F.; writing—original draft preparation, S.Y.; writing—review and editing, T.O. and A.Y.; project administration, A.O. and N.N. All authors have read and agreed to the published version of the manuscript.

Funding: This research received no external funding.

Institutional Review Board Statement: Not applicable.

Informed Consent Statement: Not applicable.

Data Availability Statement: The raw data supporting the conclusions of this article will be made available by the authors on request.

Conflicts of Interest: The authors have no conflicts of interest to declare.

 doi:10.20944/preprints202508.1235.v1

References

1. Abe, H.; Yoneda, M.; Fujiwara, N. Developments of Plasma Etching Technology for Fabricating Semiconductor Devices. Jpn. J. Appl. Phys. **2008**, 47, 1435–1455.
2. Chiappim, W.; Neto, B.B.; Shiotani, M.; Karnopp, J.; Gonçalves, L.; Chaves, J.P.; da Silva Sobrinho, A.; Leitão, J.P.; Fraga, M.; Pessoa, R. Plasma-Assisted Nanofabrication: The Potential and Challenges in Atomic Layer Deposition and Etching. Nanomaterials **2022**, 12, 3497.
3. Ryu, S.H.; Hwang, I.; Jeon, D.; Lee, S.K.; Chung, T.-M.; Han, J.H.; Chae, S.; Baek, I.-H.; Kim, S.K. Plasma-enhanced atomic layer deposition of indium-free $ZnSnO_x$ thin films for thin-film transistors. Appl. Surf. Sci. **2025**, 680, 161320.
4. Tamura, T.; Kaburaki, Y.; Sasaki, R.; Miyahara, H.; Okino, A. Direct decomposition of anesthetic gas exhaust using atmospheric pressure multigas inductively coupled plasma. IEEE Trans. Plasma Sci. **2011**, 39, 1684–1688.
5. Takamatsu, T.; Miyahara, H.; Azuma, T.; Okino, A. Investigation of reactive species using various gas plasmas. J. Toxicol. Sci. **2014**, 39, 281–290.
6. Shigeta, K.; Koellensperger, G.; Rampler, E.; Traub, H.; Rottmann, L.; Panne, U.; Okino, A.; Jakubowski, N. Sample introduction of single selenized yeast cells (Saccharomyces cerevisiae) by micro droplet generation into an ICP-sector field mass spectrometer for label-free detection of trace elements. J. Anal. At. Spectrom. **2013**, 28, 637–645.
7. Shigeta, K.; Traub, H.; Panne, U.; Okino, A.; Rottmann, L.; Jakubowski, N. Application of a micro-droplet generator for an ICP-sector field mass spectrometer – optimization and analytical characterization. J. Anal. At. Spectrom. **2013**, 28, 646–654.
8. Iwai, T.; Takahashi, Y.; Miyahara, H.; Okino, A. Development of the atmospheric plasma soft-ablation method (APSA) for elemental analysis of materials on heat-sensitive substrates. Anal. Sci. **2013**, 29, 1141–1145.
9. Miyahara, H.; Iwai, T.; Nagata, Y.; Takahashi, Y.; Fujita, O.; Toyoura, Y.; Okino, A. Elemental analysis of biological samples using atmospheric-pressure plasma soft-ablation and ICP-MS. J. Anal. At. Spectrom. **2014**, 29, 105–111.
10. Shigeta, K.; Koellensperger, G.; Rampler, E.; Traub, H.; Rottmann, L.; Panne, U.; Okino, A.; Jakubowski, N. Sample introduction of single selenized yeast cells (Saccharomyces cerevisiae) by micro droplet generation into an ICP-sector field mass spectrometer for label-free detection of trace elements. J. Anal. At. Spectrom. **2013**, 28, 637–645.
11. Yanagawa, Y.; Suenaga, Y.; Iijima, Y.; Okino, A.; Mitsuhara, I. Temperature-controlled atmospheric-pressure plasma treatment induces protein uptake via clathrin-mediated endocytosis in tobacco cells. Plant Biotechnol. **2022**, 39, 179–183.
12. Takamatsu, T.; Uehara, K.; Sasaki, Y.; Miyahara, H.; Matsumura, Y.; Iwasawa, A.; Ito, N.; Kohno, M.; Azuma, T.; Okino, A. Microbial Inactivation in the Liquid Phase Induced by Multigas Plasma Jet. PLoS ONE. **2015**, 10, e0132381.
13. Takamatsu, T.; Uehara, K.; Sasaki, Y.; Miyahara, H.; Azuma, T.; Okino, A. Investigation of blood coagulation effect of nonthermal multigas plasma jet in vitro and in vivo. Plasma Medicine. **2017**, 7, 1–12.
14. Andrae, A.S.G.; Edler, T. On Global Electricity Usage of Communication Technology: Trends to 2030. Challenges. **2015**, 6, 117–157.
15. 14. Johnsson, L.; Netzer, G. The impact of Moore's Law and loss of Dennard scaling: Are DSP SoCs an energy efficient alternative to x86 SoCs? J. Phys.: Conf. Ser. **2016**, 762, 012022.
16. Hillman, D. Integrated Power Management, Leakage Control and Process Compensation Technology for Advanced Processes. Design & Reuse. **2009**, 1–10.
17. Nowak, E.J. Maintaining the benefits of CMOS scaling when scaling bogs down. IBM J. Res. Dev. **2002**, 46, 169–180.
18. Borkar, S.; Chien, A.A. The Future of Microprocessors. Commun. ACM. **2011**, 54, 67–77.
19. Moody, G.; Islam, M.S. Materials for ultra-efficient, high-speed optoelectronics. MRS Bull. **2022**, 47, 475–484.
20. Wang, Z.; Li, X.; Ji, J.; Sun, Z.; Sun, J.; Fang, B.; Lu, J.; Li, S.; Ma, X.; Chen, X.; Zhu, S.; Li, T. Fast-speed and low-power-consumption optical phased array based on lithium niobate waveguides. Nanophotonics. **2024**, 13, 13.
21. Rani, A.; Dewra, S. Semiconductor Optical Amplifiers in Optical Communication Systems – Review. Int. J. Eng. Res. Technol. **2013**, 2, 1006–1010.
22. Duan, G.H.; Jany, C.; Le Liepvre, A.; Accard, A.; Lamponi, M.; Make, D.; Kaspar, P.; Levaufre, G.; Girard, N.; Lelarge, F.; Fedeli, J.M.; Descos, A.; Ben Bakir, B.; Messaoudene, S.; Bordel, D.; Menezo, S.; de Valicourt, G.; Keyvaninia, S.; Roelkens, G.; Van Thourhout, D.; Thomson, D.J.; Gardes, F.Y.; Reed, G.T. Hybrid III-V on Silicon Lasers for Photonic Integrated Circuits on Silicon. IEEE J. Sel. Top. Quantum Electron. **2015**, 21, 379–391.

 doi:10.20944/preprints202508.1235.v1

23. Hayashi, Y.; Suzuki, J.; Inoue, S.; Hasan, S.M.T.; Kuno, Y.; Itoh, K.; Amemiya, T.; Nishiyama, N.; Arai, S. GaInAsP/silicon-on-insulator hybrid laser with ring-resonator-type reflector fabricated by N_2 plasma-activated bonding. Jpn. J. Appl. Phys. **2016**, 55, 082701.
24. Fang, W.; Takahashi, N.; Ohiso, Y.; Amemiya, T.; Nishiyama, N. Reduced Thermal Resistance of Membrane Fabry-Perot Laser Bonded on Si Through Room-Temperature, Surface-Activated Bonding Assisted by a-Si Nano-Film. IEEE J. Quantum Electron. **2022**, 58, 2000208.
25. Maszara, W.P.; Pronko, P.P.; McCormick, A.W. Epi-less bond-and-etch-back silicon-on-insulator by MeV ion implantation. Appl. Phys. Lett. **1991**, 58, 2779–2781.
26. Takagi, H. Room-temperature wafer bonding. Surf. Sci. **2005**, 26, 82–87.
27. Hayashi, Y.; Osabe, R.; Fukuda, K.; Atsumi, Y.; Kang, J.; Nishiyama, N.; Arai, S. Low Threshold Current Density Operation of a GaInAsP/Si Hybrid Laser Prepared by Low-Temperature N_2 Plasma Activated Bonding. Jpn. J. Appl. Phys. **2013**, 52, 060202.
28. Qin, Y.; Howlader, M.M.R.; Deen, M.J. Low-Temperature Bonding for Silicon-Based Micro-Optical Systems. Photonics. **2015**, 2, 1164–1201.
29. Kikuchi, T.; Bai, L.; Mitarai, T.; Yagi, H.; Furukawa, M.; Amemiya, T.; Nishiyama, N.; Arai, S. Enhanced bonding strength of InP/Si chip-on-wafer by plasma-activated bonding using stress-controlled interlayer. Jpn. J. Appl. Phys. **2020**, 59, SBBD02.
30. Encinas, N.; Dillingham, R.G.; Oakley, B.R.; Abenojar, J.; Martínez, M.A.; Pantoja, M. Atmospheric Pressure Plasma Hydrophilic Modification of a Silicone Surface. J. Adhes. **2012**, 88, 321–336.
31. Suni, T.; Henttinen, K.; Suni, I.; Mäkinen, J. Effects of Plasma Activation on Hydrophilic Bonding of Si and SiO_2. J. Electrochem. Soc. **2002**, 149, G348–G351.
32. Ma, X.; Chen, C.; Liu, W.; Liu, X.; Du, X.; Song, Z.; Lin, C. Study of the Ge Wafer Surface Hydrophilicity after Low-Temperature Plasma Activation. J. Electrochem. Soc. **2009**, 156, H307–H311.
33. Esser, R.H.; Hobart, K.D.; Kub, F.J. Improved Low-Temperature Si–Si Hydrophilic Wafer Bonding. J. Electrochem. Soc. **2003**, 150, G228–G232.
34. Tong, Q.-Y.; Gan, Q.; Hudson, G.; Fountain, G.; Enquist, P. Low temperature InP/Si wafer bonding. Appl. Phys. Lett. **2004**, 84, 732–734.
35. Takamatsu, T.; Hirai, H.; Sasaki, R.; Miyahara, H.; Okino, A. Surface Hydrophilization of Polyimide Films Using Atmospheric Damage-Free Multigas Plasma Jet Source. IEEJ Trans. FM. **2013**, 41, 119–125.
36. Wagner, H.-E.; Brandenburg, R.; Kozlov, K.V.; Sonnenfeld, A.; Michel, P.; Behnke, J.F. The barrier discharge: basic properties and applications to surface treatment. Vacuum **2003**, 71, 417–436.
37. Yin, G.Q.; Wang, J.J.; Yuan, Q.H. The Discharge Characteristics of Capacitively Coupled Ar Plasma as the Change of Pressure. Plasma Phys. Rep. **2023**, 49, 802–807.
38. Chibowski, E.; Jurak, M. Comparison of contact angle hysteresis of different probe liquids on the same solid surface. Colloid Polym. Sci. **2013**, 291, 391–399.
39. Head, A.R.; Schnadt, J. UHV and Ambient Pressure XPS: Potentials for Mg, MgO, and $Mg(OH)_2$ Surface Analysis. JOM **2016**, 68, 3070–3077.
40. Takamatsu, T.; Hirai, H.; Sasaki, R.; Miyahara, H.; Okino, A. Surface hydrophilization of polyimide films using atmospheric damage-free multigas plasma jet source. IEEJ Trans. Fundam. Mater. **2013**, 41, 119–125.
41. Takamatsu, T.; Kawate, A.; Oshita, T.; Miyahara, H.; Okino, A.; Fridman, G. Comparison of hydrophilization effect by various gas atmospheric plasma. Proc. IEEE Int. Conf. Plasma Sci. **2011**, Abstracts, Article #5993384.
42. Takamatsu, T.; Uehara, K.; Sasaki, Y.; Miyahara, H.; Matsumura, Y.; Iwasawa, A.; Ito, N.; Azuma, T.; Kohno, M.; Okino, A. Investigation of reactive species using various gas plasmas. RSC Adv. **2014**, 4, 39901–39907.
43. Pateyron, B.; Elchinger, M.-F.; Delluc, G.; Fauchais, P. Thermodynamic and transport properties of Ar-H_2 and Ar-He plasma gases used for spraying at atmospheric pressure. Plasma Chem. Plasma Process. **1992**, 12, 421–448.
44. Hori, M. Radical-controlled plasma processes. Rev. Mod. Plasma Phys. **2022**, 6, Article 36.
45. May, E.F.; Berg, R.F.; Moldover, M.R. Reference Viscosities of H_2, CH_4, Ar, and Xe at Low Densities. Int. J. Thermophys. **2007**, 28, 1085–1110.
46. Golovicher, L.E.; Kolenchits, O.A.; Nesterov, N.A. Dynamic viscosity of gases over a wide range of temperatures. J. Eng. Phys. Thermophys. **1989**, 56, 689–694.
47. Yoshida, H.; Takei, Y.; Arai, K. Equations for Calculating the Gas Flow Rate through a Cylindrical Tube in Various Flow Regimes. Vacuum Surf. Sci. **2020**, 63, 304–310.
48. Senda, Y. Theoretical Analysis of Vacuum Evacuation in Viscous Flow and Its Applications. SEI Tech. Rev. **2010**, 176, 1–7.
49. Villarreal-Medina, R.; Murphy, A.B.; Méndez, P.F.; Ramírez-Argáez, M.A. Heat Transfer Mechanisms in Arcs of Various Gases at Atmospheric Pressure. Plasma Chem. Plasma Process. **2023**, 43, 787–803.
50. Kawata, S. Plasma Instability. Comput. Plasma Sci. **2023**, Chapter 7, 147–177.
51. Abdilla, J.; See, G.H. Chip-to-Wafer Hybrid Bonding Development for High Volume Manufacturing. IMAPSource Proceedings **2023**, Nov, Article 001c.90682.

 doi:10.20944/preprints202508.1235.v1

52. Alam, A.U.; Howlader, M.M.R.; Deen, M.J. The effects of oxygen plasma and humidity on surface roughness, water contact angle and hardness of silicon, silicon dioxide and glass. J. Micromech. Microeng. **2014**, 24, 035010.
53. Sjövall, P.; Lausmaa, J. ToF-SIMS. Encycl. Geobiol. **2009**, Chapter, 883–886.